Imaging

Imaging the right heart: the use of integrated multimodality imaging

Emanuela R. Valsangiacomo Buechel[1]* and Luc L. Mertens[2]

[1]Division of Paediatric Cardiology and Children's Research Centre, University Children's Hospital Zurich, Steinwiesstrasse 75, 8032 Zurich, Switzerland; and [2]The Labatt Family Heart Center, The Hospital for Sick Children, University of Toronto, Toronto, ON, Canada

During recent years, right ventricular (RV) structure and function have been found to be an important determinant of outcome in different cardiovascular and also pulmonary diseases. Currently, echocardiography and cardiac magnetic resonance (CMR) imaging are the two imaging modalities most commonly used to visualize the RV. Most structural abnormalities of the RV can be reliably described by echocardiography but due its complex geometrical shape, echocardiographic assessment of RV function is more challenging. Newer promising echocardiographic techniques are emerging but lack of validation and limited normal reference data influence their routine clinical application. Cardiac magnetic resonance is generally considered the clinical reference technique due to its unlimited imaging planes, superior image resolution, and three-dimensional volumetric rendering. The accuracy and reliability of CMR measurements make it the ideal tool for serial examinations of RV function. Multidetector computed tomography (MDCT) plays an important role in the diagnosis of pulmonary emboli but can also be used for assessing RV ischaemic disease or as an alternative for CMR if contra-indicated. Radionuclide techniques have become more obsolete in the current era. The different imaging modalities should be considered complimentary and each plays a role for different indications.

Keywords   Right ventricle • Multimodality imaging • Echocardiography • Cardiac magnetic resonance imaging

Introduction

The right ventricle (RV) has for a long time been the neglected side of the heart, but its role in different cardiovascular diseases has been increasingly recognized. This is obvious for structural congenital heart defects (CHD) involving the RV such as pulmonary valve stenosis, tetralogy of Fallot (TOF), and Ebstein malformation.[1] Beyond this, RV function has been shown to be one of the most important outcome determinants in patients with pulmonary arterial hypertension (PAH).[2,3] Also in patients with cardiomyopathy and ischaemic heart disease, RV dysfunction has been shown to be a strong predictor of adverse events, independent from left ventricular (LV) function and the presence of ischaemia.[4–6] Different imaging modalities can be used for imaging the RV. Due to technological advances, the role and clinical use of these techniques is evolving. In different conditions, each technique provides complementary information and this influences its use in clinical practice. Currently, echocardiography and cardiac magnetic resonance (CMR) imaging are the two most commonly used imaging techniques for structural and functional evaluation of the RV.[7] Other imaging modalities such as multidetector-computed tomography (MDCT) and radionuclide techniques are valuable alternatives in selected patients.

Right ventricular structure and function

Correct identification of the morphologic RV is the first important step for RV assessment, independently from the imaging modality used. The segmental approach to cardiac anatomy helps define the cardiac structures and segments based on constant anatomical features.[8–11] The gross anatomy of the RV differs from the LV as it has a more complex geometrical shape being 'wrapped around' the LV. This complex geometry precludes imaging the inflow and outflow tract in a single two-dimensional plane. Compared with the LV, the RV myocardium is significantly more trabeculated, and the RV wall much thinner with a normal compacted wall thickness of 3–5 mm in the adult population.

The structural organization of the myocardial cells has a characteristic complex three-dimensional myofiber arrangement.[12,13] The LV wall has a three-layered structure with the epicardial cells

* Corresponding author. Tel: +41 1 266 7339, Fax: +41 1 266 7981, Email: emanuela.valsangiacomo@kispi.uzh.ch

oriented obliquely, the mid-myocardial cells more circumferentially, and the endocardial cells again obliquely. The well-developed midwall circumferential layer is responsible for the predominance of circumferential shortening and radial thickening in the LV. The RV epicardial fibres are oriented obliquely and contiguous with epicardial LV fibres, the midwall circumferential layer is poorly developed and the endocardial fibres are oriented longitudinally. This fibre structure explains why RV ejection is determined by longitudinal shortening rather than by circumferential deformation. The normal RV contraction results in a peristaltic contraction going from the inflow to the outflow part of the RV.[14] In case of RV hypertrophy, the hypertrophied fibres seem to be oriented more circumferentially and circumferential and radial shortening contribute more to RV ejection.[15,16]

The RV is also functionally different from the LV.[17–19] Right ventricular pressure–volume loops are more triangular compared with the rectangular LV loops and have very short or absent isovolumetric contraction and relaxation periods.[18] The RV responds differently to acute and chronic stressors as well as to pharmacological agents. The RV is more sensitive to both acute and chronic pressure loading and is at risk for acute and chronic RV failure.[19] Recent data have suggested that in both ventricles, different molecular pathways are involved in the adaptive myocardial response to changes in loading conditions.[20–22] This could be related to the different embryologic origin of RV and LV myocardial cells[23,24] and has potential implications for targeted pharmacological treatment of RV failure.

Interventricular interaction is another important aspect of RV disease: RV hypertrophy and/or dilatation affect LV function.[25–28] The increased transseptal gradient associated with RV hypertension causes bowing of the interventricular septum towards the LV. In RV dilatation, this occurs during diastole influencing LV filling, and in the case of elevated RV systolic pressure, this can affect LV systolic function and mechanics. Thus, RV abnormalities may indirectly affect LV output and overall cardiac performance.

Imaging modalities

Echocardiography

Right ventricular morphology can generally be adequately described by transthoracic echocardiography in most patients. Only when transthoracic imaging windows are poor and RV disease is suspected, additional imaging may be required. Depending on patient age and clinical problem, transoesophageal echocardiography, CMR, or MDCT can be used.

Assessment of RV size and function should be part of every echocardiographic examination at the time of first diagnosis and during serial follow up, particularly in patients with chronic conditions, such as PAH and cardiomyopathy. Guidelines for the echocardiographic evaluation of the RV have been published for the adult[29] and paediatric population.[30] Both guidelines stress the importance of combining different 2D echocardiographic views for obtaining full coverage of the different RV segments. Different apical views as well as subcostal and parasternal long-axis and short-axis views should be acquired (*Figure 1*). Echocardiographic evaluation should also include 2D measurements of right atrial dimensions and RV wall thickness. The most commonly used normal values for the adult population reported in the echocardiographic guidelines as a summary of several studies are shown in *Table 1*. These proposed normal data have some limitations: the reproducibility of different measurements needs to be tested and the normal data will have to be stratified for age ranges, body size, and gender. Assessment of RV volumes using 2D echocardiography is more challenging. Two-dimensional RV measurements as well as different geometrical formula proposed for volume calculation
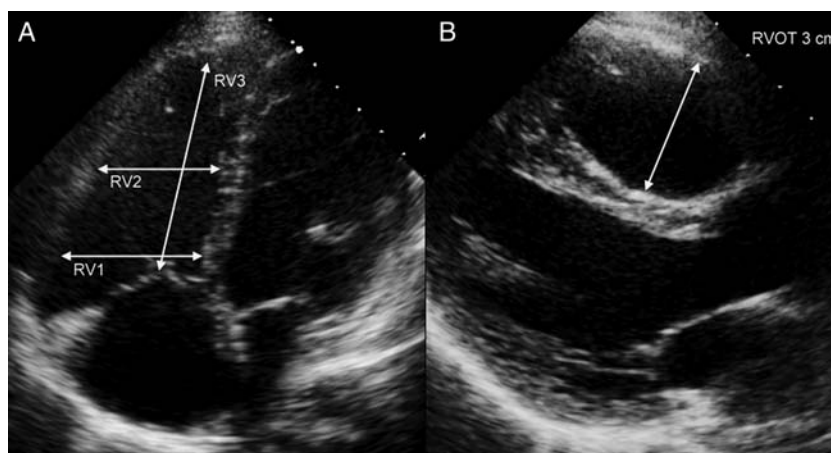
Figure I Measurement of right ventricular (RV) dimensions using echocardiography. Two-dimensional measurements should be made in different parts of the RV. (*A*) From the apical four-chamber view, the inflow part of the RV is measured as the maximal short-axis dimension in the basal one-third of the RV (RV1). The midcavity dimension is measured in the middle third of the RV at the level of the papillary muscles (RV2). This represents the trabecular part of the RV. The longitudinal dimension is measured from the middle of the tricuspid valve to the RV apex (RV3). (*B*) From the parasternal long-axis view, the proximal part of the right ventricular outflow tract is measured.

Table 1   Two-dimensional measurements of the right ventricular cavity

	Normal value	Limitation
2D RV measurements		
RV 1 (RV basal diameter)	<4.2 cm	Influenced by probe rotation Requires RV-focused view
RV 2 (midcavity diameter)	<3.5 cm	Level of measurement not clearly defined (level LV papillary muscles) Normal value?
RV 3 (base-apex RV length)	<8.6 cm	Influenced by probe rotation Definition of RV apex?
RV end-diastolic area	<28 cm^2	Influenced by probe rotation Definition of trabeculations can be difficult
RVOT parasternal short axis just proximal to pulmonary valve	2.7 cm	Often difficult endocardial definition Limited normative data
RVOT parasternal long axis	3.3 cm	Anterior wall definition can be difficult Limited normative data
2D right atrial dimensions		
RA major dimension (apical 4C)	<5.3 cm	Influenced by imaging plane Relatively few normative data
RA minor dimension	<4.4 cm	Imaging plane will affect measurement
RA end-systolic area	<20 cm^2	Few normative data

Table 2   Right ventricular functional measurements

Measurement	Normal value	Limitation
%FAC	>35%	Endocardial border detection can be difficult especially in systole Load-dependent No imaging of the outflow tract
TAPSE	>16 mm	Influenced by direction of motion (alignment) Influenced by loading and tricuspid regurgitation No imaging of the outflow tract
Peak systolic tissue Doppler velocity tricuspid annulus	>10 cm/s	Influenced by alignment with the motion Influenced by loading conditions Only one single segment used for global function
Peak systolic longitudinal strain of the RV lateral wall	No good reference value	Needs further validation Normative data are needed

FAC, fractional area change; TAPSE, tricuspid annular plane excursion.

show poor agreement with three-dimensional (3D) volumes calculated by CMR.[31,32] Recently, 3D echocardiography has emerged as a promising technique for the assessment of RV volumes.[33] Different methods have been proposed for the analysis of 3D volumetric data sets; the most commonly used being the Beutel technique.[34–38] This method has been proven to be reliable and accurate in different conditions, including CHD and PAH. The challenge of acquiring a good quality full volumetric 3D data set, including the RV anterior wall and the RV apical lateral segments, in patients with poor imaging windows and/or dilated RV is the main limitation of the method. Moreover, accuracy tends to decrease with increasing RV dilatation, limiting its application in the more dilated ventricles.[34,39] Three-dimensional echocardiography can also be useful for imaging the tricuspid valve, as all three leaflets and commissures

can be visualized in a single 3D image. The mechanisms of tricuspid regurgitation can be better understood, which facilitate guiding surgical repair.[40–42]

Due to the limitations discussed above, echocardiographic assessment of RV function remains challenging in clinical practice and often is limited to subjective qualitative assessment. Recent guidelines recommend performing quantitative measurements of RV function[29,30] by using at least one of the following echocardiographic parameters as surrogate of volumetric assessment of RV function: percent fractional area change (FAC), tricuspid annular plane systolic excursion (TAPSE), or RV index of myocardial performance (RIMP) (Table 2). The observation that the combined use of three different parameters is being proposed probably indicates that no single measurement has been validated for clinical use
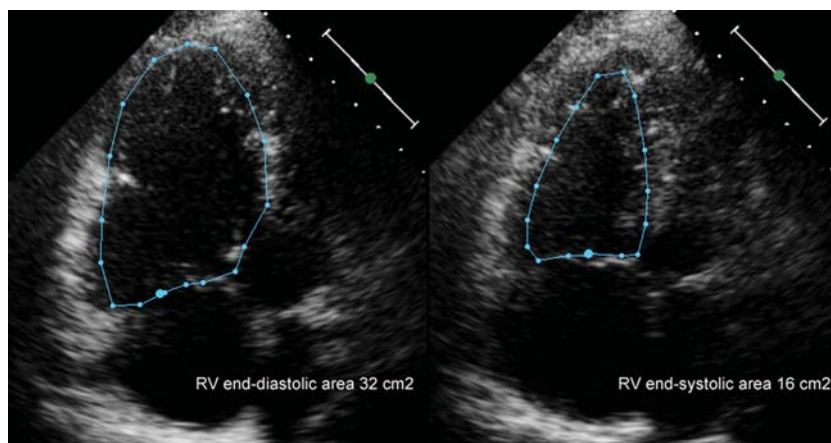
Figure 2 Measurement of fractional area change (FAC). Right ventricular end-diastolic and end-systolic area is measured from an apical four-chamber view. FAC is calculated as (end-diastolic area-end-systolic area)/end-diastolic area. In the example shown FAC is 50% (normal value >35%).
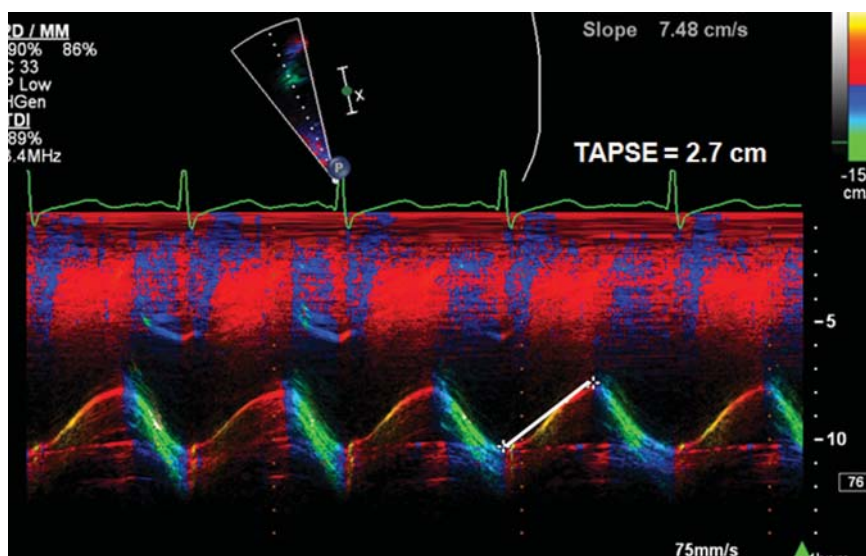

Figure 3 Tricuspid annular planar systolic excursion (TAPSE). From the apical four-chamber view, an M-mode is put through the tricuspid annulus with as good alignment as possible with longitudinal motion of the annulus. The systolic displacement of the tricuspid annulus is measured. To optimize timing, we use tissue colour M-mode which allows to well define end-diastole and end-systole on the tracings. TAPSE should be >1.6 cm.

in different conditions and that their impact on management and outcome remains uncertain.

Fractional area change (*Figure 2*) has been shown to correlate with RV EF calculated by CMR and to be an independent predictor for outcome after myocardial infarction.[43] However, image quality and visualization of the endocardial borders are often limited especially in the RV lateral wall and RV apex. Tricuspid annular plane systolic excursion (*Figure 3*) is easy to measure and represents longitudinal shortening of the RV lateral wall, but normal values for different age groups and its validation are limited.[29] In addition,

the presence of tricuspid regurgitation may influence the values obtained. Right ventricular index of myocardial performance is a Doppler method combining measurement of isovolumic contraction and relaxation times.[44] Right ventricular index of myocardial performance is load dependent and due to the short RV isovolumic time intervals, its use remains controversial.[45]

Emerging echocardiographic techniques like tissue Doppler (TDI) and strain imaging have been applied to the assessment of RV function. Peak tissue Doppler systolic velocity in the tricuspid annulus is a measurement of RV longitudinal function (*Figure 4*).
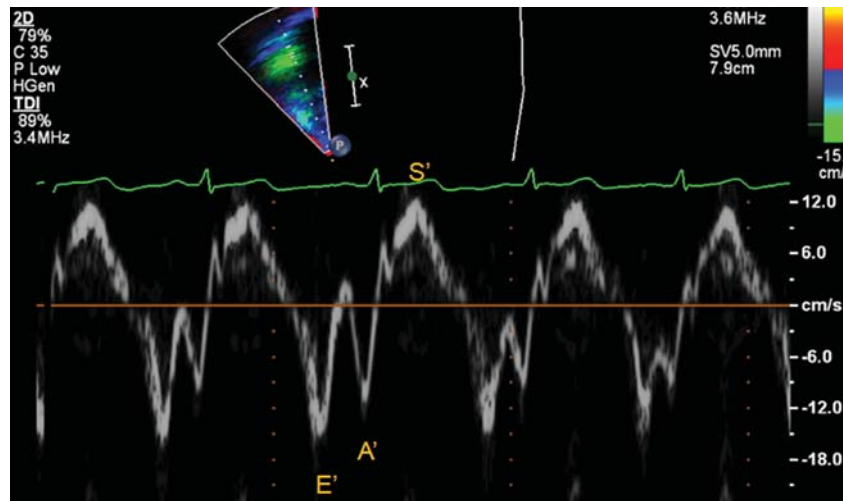
Figure 4 Pulsed tissue Doppler of the tricuspid annulus. This a pulsed Doppler tracing obtained in the tricuspid annulus from the apical four-chamber view. A systolic peak velocity (S′), early diastolic velocity (E′), and atrial contraction velocity (A′) can be measured. Notice on this trace the near absence of isovolumetric periods in this normal right ventricle. After systole, the early diastolic wave starts, after diastolic, during the isovolumetric period there is a short isovolumetric peak corresponding to changes in the myocardium during the isovolumetric period.
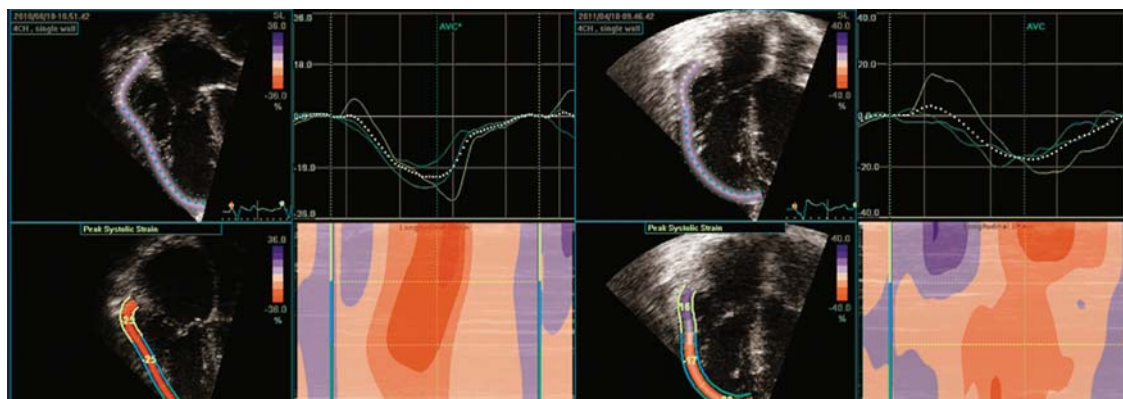
Figure 5 Longitudinal strain measurement in the right ventricular (RV) free wall. From the apical four-chamber view, strain curves are obtained using speckle tracking echocardiography. On the left panel, strain in the RV free wall was measured in a postoperative tetralogy of Fallot patient. This patient underwent pulmonary valve replacement and the right-hand panel reflects strain measurements 6 months after the surgery. A reduction in strain may result from changes in RV stroke volume, RV preload, and RV geometry.

This technique is easy and reproducible but has the limitations of being angle-dependent, load-dependent, and influenced by the global cardiac translation and tricuspid regurgitation. In the young adult, a normal cut-off value of ≥10 cm/s has been proposed; however, normal data for all different age ranges and gender are lacking.[29]

The introduction of speckle-tracking echocardiography made the measurement of strain and strain rate easier. Although developed for the LV, speckle tracking has been applied to the RV.[7,46] Peak longitudinal strain and strain rate measurement are independent from global cardiac motion and allow quantifying regional myocardial deformation in the different RV segments. Right ventricular strain has been shown to be reduced in patients with PAH,[25,47,48] a systemic RV,[49,50] and after TOF repair[51,52] (*Figure 5*). Although very promising, myocardial deformation imaging has significant limitations. Strain values are influenced by loading conditions, as it has been demonstrated in patients with PAH, in whom RV longitudinal strain was related to pulmonary arterial systolic pressures.[25] Additionally, strain values are influenced by RV size and stroke volume. Feasibility is not always given in the thin RV wall; normal values for different age ranges, body size, and gender still have not been established yet; standardization among different software solutions is still being investigated. Therefore, TDI and speckle tracking are not ready yet for routine clinical use.[53]

Cardiovascular magnetic resonance

Cardiovascular magnetic resonance is the second-line modality after echocardiography for comprehensive RV evaluation. Cardiovascular magnetic resonance is currently considered the reference standard for functional RV studies as it allows visualizing anatomy, quantifying function, and calculating flows.

Anatomical assessment is usually performed with T1-weighted black-blood turbo spin-echo sequence or with the steady-state free precession (SSFP) sequence. Standard axial images allow segmental analysis of cardiac anatomy and visualization of the pulmonary arteries, pulmonary veins, aorta, and systemic veins. Detailed description of the intra- and extracardiac anatomy can be achieved by 3D rendering techniques, including contrast-enhanced MR angiography and 3D SSFP. This is important for detailed description of complex cardiac anatomy and for preoperative planning.[54,55]

Cardiovascular magnetic resonance also provides advanced imaging of the RV myocardium inclusive tissue characterization. Different T1- and T2-weighted sequences combined with late-enhancement imaging after gadolinium administration can be used for tissue characterization. Tissue characterization is used for assessment and differentiation of different cardiomyopathies affecting the RV, including arrhythmogenic RV cardiomyopathyopathy (ARVC), metabolic storage diseases, and cardiac tumours.[56–59] Late enhancement imaging shows intramyocardial fibrosis, inflammation, scars, and fat accumulation (Figure 6). In CHD, the presence of myocardial scars in the RV is supposed to be a risk factor for adverse events during follow-up.[60,61] Interpretation of the images can be challenging due to the thin RV wall and the surrounding epicardial fat and pericardium. The prognostic significance of myocardial late-enhancement in various diseases needs further investigation.

Figure 6 Late gadolinium enhancement in the right ventricular free wall. Late enhancement indicating fibrosis of the right ventricular and left ventricular myocardium (arrows) in a patient with Naxos disease, a disease associated with right ventricular arrhythmogenic ventricular dysplasia.

Cardiovascular magnetic resonance is considered the clinical reference technique for accurate assessment of global RV function. Short-axis or axial SSFP images and the summation disc method are used for calculation of RV volumes and ejection fraction (EF) without any geometrical assumption (Figure 7). Appropriate spatial and temporal resolution of the images is important for accuracy of the results and can be achieved by adjusting acquisition parameters to the patient's size and heart rate.[62] Normal age- and gender-specific values for RV volumes and function have been published for the adult and the paediatric population.[63,64] Provided adequate standardization, CMR RV measurements show high reproducibility with an interobserver variability <7% for the end-diastolic volume, <14% for the end-systolic volume, <7% for EF, and <20% for RV mass.[63–67] Right ventricular segmentation is more challenging than LV segmentation and variability of the data can be influenced by sternal wires obscuring the RV anterior wall, correct identification of the level of tricuspid and pulmonary valve, the thin RV wall, the complex trabeculated RV cavity, and the partial volume effect in the RV apex.[64] Axial acquisition of the images has been reported to improve accuracy of the measurements,[68] but normal data are only available for children.[65,68]

Regional RV function can be evaluated qualitatively at rest and during pharmacological stress on SSFP short-axis cine loops.[69] Regional dysfunction can be assessed quantitatively by using myocardial tagging or strain encoding CMR; both techniques have been shown to be feasible in the RV correlate well with echocardiographic evaluation.[70,71] However, their application in the RV is technically demanding, due to the thin wall, and extensive post processing, limiting their clinical application.[72]

Velocity-encoded phase contrast imaging is another important CMR tool for RV evaluation. Phase contrast imaging enable quantification of RV stroke volume, pulmonary and/or tricuspid valve regurgitation, intracardiac shunts as well as of differential lung perfusion.[73–75]

Multidetector computed tomography

Multidetector computed tomography is not a routinely used technique for RV assessment, due to the significant radiation exposure and the use of iodinated contrast medium.[76] Multidetector computed tomography is usually performed when concomitant thoracic or pulmonary disorders, such as pulmonary embolism (PE), are suspected. Multidetector computed tomography is a valuable alternative to CMR in patients with pacemaker, CMR incompatible prosthetic material and claustrophobia. Recent improvements in temporal and spatial resolution affected cardiac visualization.[76] The use of MDCT for the RV has mainly been validated for the detection of PE and for work up of pulmonary hypertension.[77] Multidetector computed tomography is increasingly used for detecting coronary artery disease as its accuracy has been demonstrated for non-invasive visualization of both coronary arteries.[78,79] Recently, radiation dose could be importantly reduced also in comparison to diagnostic coronary angiography.[80]

Structural evaluation of the RV by MDCT includes measurement of RV size and volumes, as well as RV free myocardial wall thickness (RV hypertrophy). Septal bowing into the LV indicates RV volume (diastolic bowing) or pressure overload (systolic bowing).
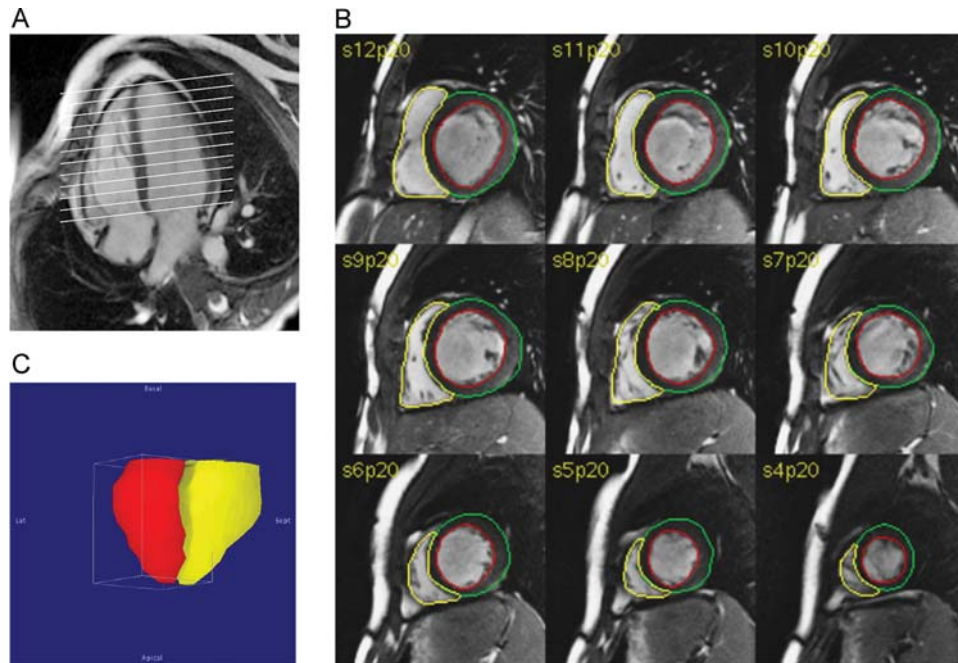
Figure 7 Measurement of right ventricular (RV) volume and function by SSFP. (*A*) A stack of 10–12 adjacent slices are acquired on a vertical long-axis view showing both atria and both ventricles. (*B*) Endocardial contours (yellow line for RV, red line for LV, green line for LV epicardium) of each ventricle are traced in the end-systolic and end-diastolic phase during postprocessing. (*C*) Data analysis is performed with the summation disc method, which provides the real shape of the right ventricle (yellow).

The diameters of the systemic veins and pulmonary arteries are indirect measures of elevated preload and afterload, respectively.[81] Normal values for RV structures measured by MDCT have been recently published.[82] ECG-gating during image acquisition is needed for functional assessment and for CT angiography of the coronary arteries. Therefore, beta-blockers are usually administered in patients with heart rate >75 per min for optimizing image acquisition.[76] Compared with CMR, MDCT has lower temporal resolution and tends to overestimate end-systolic and end-diastolic volumes.[83]

Radionuclide techniques

Radionuclide techniques have historically been the first modalities used for assessing RV function.[84] They have largely been replaced by CMR and echocardiography. Nonetheless, radionuclide modalities still play a role in assessment of RV myocardial ischaemia and in patients in whom CMR is contraindicated.[85] Among different techniques tested, gated blood-pool single photon emission computed tomography (SPECT) is the currently recommended nuclear modality for quantifying RV function, as its 3D nature overcomes the common limitations of other nuclear techniques.[84,86] Gated SPECT is able to provide RV volumetric and functional data,[87] but further studies for validation of automatic measurement algorithms are still pending.

Radionuclide techniques are of additional particular interest for assessing myocardial metabolism and perfusion. The use of positron emission tomography (PET) or SPECT for RV evaluation is in general limited by the lower overall counts attributable to the RV compared with the LV causing inconsistent RV visualization.[84] In the pathologic RV, hypertrophy leads to an increased RV tracer uptake and results in improved RV visualization. In PAH, changes in RV myocardial metabolism and perfusion are thought to be a precursor of deterioration of systolic function, RV failure, and/or clinical symptoms, and may be used for guiding therapeutic decision making.[85] Experimental studies using SPECT have shown that acute or chronic RV pressure overload leads to a myocardial metabolic shift from fatty acid to glucose.[88] Positron emission tomography may be superior to SPECT for visualization of the RV, due to its superior spatial resolution and attenuation correction. More recently, 18F-fluorodeoxyglucose PET has been utilized to assess response to epoprostenol therapy in PAH patients.[89]

Finally, new hybrid SPECT/CT and PET/CT systems are being used in the LV for assessing myocardial perfusion, metabolism, function, and anatomy (coronary arteries) in one single examination. Their feasibility in the RV still needs to be demonstrated.[90]

Clinical application of non-invasive imaging in conditions affecting the right ventricle

Pulmonary arterial hypertension

Echocardiography plays an important role in the clinical detection of PAH and in the diagnostic work-up of some of its causes like

left-sided heart disease or CHD. In patients with PAH at the time of first diagnostic work up, MDCT is an established modality for exclusion of pulmonary tissue disease, vascular disease, and PE.[77,91] Cardiovascular magnetic resonance adds information about flow velocities and profiles in the pulmonary arteries and veins.

Right ventricular function has been shown to be an important predictor of survival in patients with PAH.[92,93] The increased after-load caused by the increased pulmonary vascular resistance causes RV hypertrophy and remodelling. With the progression of the disease, the hypertrophic response becomes inadequate and can be associated with pathological changes, such as progressive RV myocardial fibrosis and dysfunction. Different echocardiographic measurements have been shown to have prognostic value in patients with PAH and are summarized in Table 3. Right atrial and RV size, %FAC, and TAPSE[26,94] are good parameters for monitoring the therapeutic effect of pulmonary vasodilator treatment. Three-dimensional echocardiography has been proposed for monitoring progressive RV dilatation as a marker for disease progression.[95] The effects of vasodilator therapy could be monitored by CMR, as RV volume, function, and mass can be measured more reliably and RV output can be calculated with two different techniques (volumetry and blood flow). Cardiac magnetic resonance has a higher sensitivity for detecting serial changes.[96] The limited accessibility and cost are probably the main reason why it is not routinely used for follow-up in most centres. Recent CMR studies demonstrated a high incidence of fibrotic areas in the RV myocardium in PAH patients. This finding suggests that a pathological fibrotic response may contribute to progressive RV failure

in these patients.[97] Recent echocardiographic studies suggested that RV apex function may be affected more significantly than other RV segments.[98] All these data show how multimodality imaging of the RV plays an important role in the diagnosis and management of patients with PAH.

Multidetector computed tomography has become the most important imaging test in the diagnosis of acute PE.[91] Due to its very high negative predictive value (around 95%), MDCT can be used practically as a stand-alone test for the exclusion of acute PE.[99] Whereas scintigraphy is still used as the main screening tool for evaluation of chronic thromboembolic pulmonary hypertension, in an acute setting and in most centres MDCT has replaced ventilation−perfusion scanning because of the high number of inconclusive results of the latest.[100] Echocardiography has a low sensitivity in diagnosing PE (60−70%) and is mainly used for risk stratification.[101] The echocardiographic criteria suspicious for PE include RV dilatation, hypokinesis, and signs of pulmonary hypertension such as increased tricuspid regurgitation velocity.[91] Patients with RV dysfunction related to PE have been shown to be at higher risk for early mortality.[102]

Ischaemic right ventricular disease and right ventricular failure

Although isolated RV myocardial infarction is extremely rare, RV ischaemia complicates up to 50% of inferior myocardial infarctions.[103] In acute RV ischaemia, RV free wall hypokinesia or akinesia detected by echocardiography is a qualitative and sensitive parameter for RV dysfunction,[104] and in combination with RV

Table 3 Prognostic value of echocardiographic measurements in pulmonary hypertension

Imaging parameter	Predictive value	Limitation
Right atrial size indexed for height[136]	Increase in 5 cm^2/m increases the hazard for death by 1.54 (95% confidence interval: 1.13−2.10)	Variability in imaging of the RA
RV diameter[137]	36.5 mm - death rate increase from 6.6/100 person years (diameter <36.5 mm) to 15.9/100 person years (diameter >36.5 mm)	Needs further validation
Myocardial performance index[138]	Normal 0.28 ± 0.04	No cut-off value
	Predictor of adverse outcome (increase by 0.1 unit increases the hazard ratio 1.3; 95% confidence interval :1.09−1.56)	Influenced by loading conditions
TAPSE[3]	Cut-off value 1.8 cm	Angle-dependent
	For every 1 mm decrease in TAPSE, the unadjusted risk of death increased by 17% (hazard ratio, 1.17; 95% confidence interval 1.05−1.30)	Influenced by overall cardiac motion
Pulmonary vascular capacitance (stroke volume/pulse pressure)[139,140]	Systolic PA pressure from TR-jet; diastolic pressure from PR-jet and stroke volume from LVOT measurement	Difficult to measure requires: TR-jet; PR-jet; good LVOT alignment
	Strong independent predictor of mortality	
	Risk ratio 3.0/mL/mm Hg decrease in PVCAP (95% confidence interval 1.2−8.0)	
Average free RV wall systolic longitudinal strain[141]	Cut-off: >−12.5%	Further standardization required
	A 2.9-fold higher rate of death per 5% absolute decline in RV free wall strain at 1 year	

LVOT, left ventricular outflow tract; PR, pulmonary regurgitation; PVCAP, pulmonary vascular capacitance; RA, right atrium; TAPSE, tricuspid annular plane excursion; TR, tricuspid regurgitation.

dilatation defines RV myocardial infarction (RVMI).[105] Additional features of RV involvement include paradoxical septal motion due to increased RV end-diastolic pressure, tricuspid regurgitation, and severe RA enlargement with possible leftward deviation of the interatrial septum. Tricuspid annular plane systolic excursion has been shown to have prognostic value in patients with congestive heart failure, but its significance in acute RVMI is unclear. Tissue Doppler studies have demonstrated reduced systolic lateral tricuspid velocities in patients with concomitant RVMI and with ischaemic RV diastolic dysfunction.[106] Recently, the combined used of lateral tricuspid annulus velocities and RVMPI has been suggested for detecting RV dysfunction in RVMI in the acute and late phase.[107]

Cardiac magnetic resonance is being increasingly used for diagnosis and assessment of RV ischaemia. T2-weighted sequences can depict myocardial oedema and late gadolinium enhancement suggests fibrosis after RVMI.[108–110] A multicentre prospective study demonstrated that early postinfarction RV ischaemic injury is common and is characterized by the presence of myocardial oedema, late gadolinium enhancement, and functional abnormalities. Right ventricular injury is not limited to inferior infarcts but also occurs in anterior infarcts. During follow-up, RV dysfunction may be reversible and permanent myocardial damage limited.[59] Late after myocardial infarction, CMR evaluation of RV function can be used for risk-stratification and refined management of these patients, as RVEF is an important predictor of prognosis.[111]

In suspected CAD, MDCT enables accurate visualization of the coronary arteries, not only of the left but also of the right coronary artery.[79] Compared with invasive coronary angiography, new generation MDCT offer equal high accuracy but delivers a significantly lower radiation dose to the patient.[80]

In patients with congestive heart failure, decreased RV function has been found to be a critical prognostic factor, in addition to clinical parameters, such as NHYA class and exercise performance.[6,112] Identification of the cause for dilated cardiomyopathy is crucial for clinical management and guiding treatment. Ischaemic cardiomyopathy can be accurately ruled out by MDCT, nuclear techniques, and/or by CMR.[79] Different late enhancement pattern at CMR is indicative for different non-ischaemic causes of cardiomyopathy, including myocarditis, cardiac amyloidosis, sarcoidosis, Anderson−Fabry disease, and other storage diseases.[58,113,114]

In summary in ischaemic RV disease and RV failure, the different imaging modalities provide complementary information. Echocardiography is used for basic evaluation and routine follow-up of RV function, CMR helps distinguish between non-ischaemic and ischaemic RV failure and show myocardial oedema and scars after myocardial infarct, MDCT provides accurate non-invasive imaging of the coronary arteries.

Arrhythmogenic right ventricular dysplasia

Arrhythmogenic RV cardiomyopathyopathy is a typical myocardial disorder affecting primarily the RV. In the early stages of the disease, structural changes may be subtle or absent and confined to a localized region of the RV, typically within the so-called
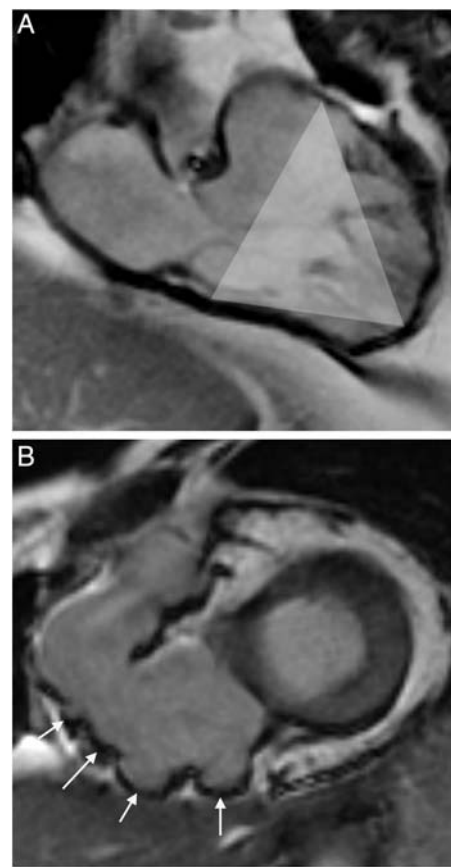
Figure 8 The triangle of dysplasia in arrhythmogenic right ventricular (RV) cardiomyopathyopathy (ARVC). (*A*) Structural anomalies can be observed in a region including the subtricuspidal RV wall, the RV apex, and the RV outflow tract. (*B*) Steady-state free precession images showing severe aneurysmatic abnormalities of the RV free wall subtricuspidal (arrows) in a patient with ARVC.

triangle of dysplasia (*Figure 8*). As ventricular arrhythmia can occur anytime, affected patients are at risk for sudden death and timely diagnosis can help preventing arrhythmias and sudden death.[115]

The most recent Task Force Criteria (TFC) for diagnosis of ARVC include global or regional structural and functional alterations, histopathologic tissue characterization, ECG abnormalities, arrhythmias, and family history.[57] Echocardiography and CMR are the proposed imaging modalities for assessing structural and functional criteria as shown in *Table 4*. Echocardiographic abnormalities of the RV can be found in up to 62% of subjects.[116] Dilatation of the RV outflow tract (RVOT) occurs in all positive subjects and global RV dysfunction is observed in more than two-thirds. Measurement of RVOT dimension in the parasternal long-axis or short-axis view should be included in each echocardiographic screening examination, as regional RV enlargement can be missed in the apical four-chamber view. Additional abnormalities consist of RV regional wall motion abnormalities, abnormal trabeculations, hyperreflective moderator band, and sacculations of the RV free

Table 4   Imaging task force criteria for diagnosing arrhythmogenic right ventricular cardiomyopathyopathy

Structural and functional criteria for ARVC

Major criteria

2D echo	Regional RV akinesia, dyskinesia, or aneurysm
	And 1 of the following (end-diastole):
	RVOT $\geq$32 mm (19 mm/m^2)/parasternal long-axis view
	RVOT $\geq$36 mm (21 mm/m^2)/parasternal short-axis view
	or RV fractional area change $\leq$33%
CMR	Regional RV akinesia or dyskinesia, or dyssynchronous RV contraction
	And 1 of the following:
	RV end-diastolic volume $\geq$110 mL/m^2 (male) or $\geq$100 mL/m^2 (female)
	or RV ejection fraction $\leq$40%

Minor criteria

2D echo	Regional RV akinesia or dyskinesia
	And 1 of the following (end-diastole):
	RVOT $\geq$29 mm <32 mm ($\geq$16 <19 mm/m^2)
	RVOT $\geq$32 <36 mm ($\geq$18 <21 mm/m^2)
	or fractional area change >33 to $\leq$40%
CMR	Regional RV akinesia or dyskinesia, or dyssynchronous RV contraction
	And 1 of the following:
	RV end-diastolic volume $\geq$100 <100 mL/m^2 (male) or $\geq$90 <100 mL/m^2 (female)
	or RV ejection fraction >40 $\leq$45%

Adapted from: Marcus *et al*.[57] Proposed modification of the Task Force Criteria.
RVOT, RV outflow tract.

wall.[116] Tissue Doppler evaluation of myocardial velocities and 3D echocardiography may be helpful in the early non-invasive diagnosis of ARVC.[117,118] Cardiac magnetic resonance adds information to echocardiography, as it enables visualization of subtle changes and of remote RV segments, such as the RV infero-posterior wall; RV volumes and function can be quantified (*Table 5*). Qualitative criteria such as segmental RV dilatation, presence of RV microaneurysms, or fatty infiltration have been removed from the revised TFC, as they have been shown to have low sensitivity and specificity.[57,119,120] Similar qualitative findings were observed in patients with benign RVOT arrhythmias in the absence of ARVC. Fatty infiltration can be found in normal heart as well.[115]

In summary, each imaging modality should not be used in isolation as an independent marker. The combined use of echocardiography and CMR adds a powerful and accurate piece of information for the diagnosis of ARVC.

Congenital heart disease

In CHD, the RV is frequently exposed to a chronic volume or pressure overload. This is the case in intracardiac shunts (atrial septal defect), anomalies of the pulmonary valve, and arteries (pulmonary atresia) and when the RV is pumping in the systemic circulation (transposition of the great arteries, single ventricle). Eventually, RV function is the main determinant of prognosis in these patients. Tetralogy of Fallot is the most common cyanotic CHD and a good example on how multimodality imaging of the RV can be used in CHD. Surgical repair of TOF provides excellent survival, but residual lesions are frequent and determine long-term morbidity

and mortality.[121] Echocardiography correctly identifies the presence of a residual ventricular septal defect, RVOT obstruction, and pulmonary regurgitation. In TOF patients, 2D echocardiographic measurements of the RV correlate only moderately with RV end-diastolic volume (RVEDV) as measured by CMR.[31,122] The strongest relationship is found between RV end-diastolic area from the apical four-chamber view and RVEDV.[122] Right ventricular systolic function can be estimated using % FAC, TAPSE, and tricuspid annular tissue Doppler velocities. Three-dimensional echocardiography is emerging and may be able to replace CMR-based volumetric measurements at least in patients with a good imaging window.[34] Diastolic dysfunction in restrictive RV physiology is demonstrated, if a late diastolic (during atrial contraction) antegrade flow in the pulmonary artery is shown at Doppler echocardiography.[123] Restrictive RV physiology has been found to have a protective role against progressive RV dilatation and to better predict exercise performance late after TOF repair, although this could only be observed in an adult cohort and is more controversial at younger age.[123]

Chronic pulmonary valve regurgitation after TOF repair leads to progressive RV dilatation and dysfunction. Right ventricular volume measured by CMR has become an important parameter for trying to determine the ideal timing for pulmonary valve replacement.[66,124,125] Oosterhof *et al*.[126] found that a RVEDV <160 mL/m^2 and a RV end-systolic volume <82 mL/m^2 are predictive for normalization of RV dimensions after pulmonary valve replacement. In TOF patients, CMR is considered the ideal tool for serial assessment of RV volumes before and after pulmonary valve replacement.[66]

Table 5 Summary of the right ventricular parameters that can be assessed by specific and/or combined imaging modalities in various diseases

Measurements	Imaging modality	Disease
RV anatomy	Echocardiography CMR (SSFP) MDCT	All CHD
RV dimensions	2D echocardiography CMR (SSFP, volumetry) MDCT	All CHD ARVC (RVOT)
Pulmonary valve	Echocardiography CMR (phase contrast imaging for regurgitation quantification)	CHD
Pulmonary arteries	CMR (angiography/3D SSFP) MDCT Echocardiography (proximal segments)	CHD PAH, pulmonary embolism
Tricuspid valve	Echocardiography 3D echocardiography	All
RV volumes	CMR (SSFP)	All
RV ejection fraction	Echocardiography (2D/3D) Gated blood-pool SPECT MDCT	
Regional RV function	Tissue Doppler imaging	All
Myocardial velocities	Speckle tracking	
Strain/strain rate (investigational)	CMR (tagging, velocity encoded sequences)	
RV ischaemia	CMR (late enhancement, oedema) Echocardiography (wall motion) SPECT (perfusion)	RV ischaemic disease RV failure
RV scars/fibrosis	CMR (late enhancement) SPECT	RV failure RV ischaemic disease Myocarditis CHD
Coronary arteries	MDCT PET/CT	RV ischaemic disease

The imaging modalities are represented in the order they should be performed for the specific wanted measurement.
ARVC, arrhythmogenic right ventricular cardiomyopathy; CHD, congenital heart disease; CMR, cardiovascular magnetic resonance; MDCT, multidetector computed tomography; RVOT, right ventricular outflow tract; PAH, pulmonary arterial hypertension; PET, positron emission tomography; SPECT, single-photon electron-computed tomography; SSFP, steady-state free precession sequence.

More recently, regional myocardial RV function has been used for advanced functional assessment after TOF repair. Impaired longitudinal RV deformation indices have been described in the presence of pulmonary regurgitation by TDI and speckle tracking.[51,127] Interestingly, progressive deterioration of RV longitudinal strain has been found in patients with stable EF, suggesting that myocardial strain could be a more sensitive parameter for detecting early ventricular dysfunction.[51,128] Acute improvement of longitudinal RV and septal function could be demonstrated by speckle tracking after percutaneous pulmonary valve replacement.[129] Velocity-encoded CMR imaging of RV myocardium provides similar myocardial velocities and timing of velocities as TDI. Peak systolic velocities in the RV free wall and in the RVOT are reduced in TOF patients compared with normals.[130]

The importance of the infundibulum has been investigated by looking at the segmental function in different RV regions, distinguishing between the RV inlet, the trabeculated apical part, and the RV outlet. Not surprisingly, EF is predominantly reduced in the outlet part where the surgical patch has been inserted.[131] This reduced myocardial deformation in the infundibular region correlates well with areas of late enhancement as well as with global EF.[132]

Cardiac magnetic resonance provides important additional information, including calculation of pulmonary regurgitant volume and fraction,[73] measurement of differential lung perfusion,[133] and late-enhancement imaging.[61] The presence of RV myocardial scars has been reported to have prognostic relevance in TOF patients, as it correlates with RV size, function, length of QRS complex at ECG, and may predict ventricular arrhythmias.[134] Contrast-enhanced MR angiography or 3D SFFP provides exact anatomical evaluation of the RVOT and the pulmonary arteries and is helpful for planning reinterventions[55] particularly for selecting patients for percutaneous pulmonary valve replacement.[135]

Conclusions

The significance of RV function is being increasingly recognized in the acute phase and during follow-up as prognostic factor in

several cardiac diseases. Echocardiography and CMR are the imaging modalities of choice for imaging the right heart. In most patients, both techniques provide complementary information and can be used in combination for almost complete evaluation of the RV. Multidetector computed tomography and nuclear imaging technique are valuable alternative modalities and add important additional information in selected cases, particularly in RV ischaemic disease. Emerging new technologies such as 3D echocardiography, TDI, speckle tracking as well as new CMR sequence are enlarging the spectrum of the pathophysiologic information obtained, but are still confined to investigational use and need further clinical validation. *Table 5* summarizes the use of all these imaging modalities for assessing the different RV parameters in various diseases, and may serve as guide for multimodality imaging.

Acknowledgements

References

1. Warnes CA. Adult congenital heart disease: importance of the right ventricle. *J Am Coll Cardiol* 2009;**54**:1903–1910.
2. D'Alonzo GE, Barst RJ, Ayres SM, Bergofsky EH, Brundage BH, Detre KM, Fishman AP, Goldring RM, Groves BM, Kernis JT *et al.* Survival in patients with primary pulmonary hypertension. Results from a national prospective registry. *Ann Intern Med* 1991;**115**:343–349.
3. Forfia PR, Fisher MR, Mathai SC, Housten-Harris T, Hemnes AR, Borlaug BA, Chamera E, Corretti MC, Champion HC, Abraham TP, Girgis RE, Hassoun PM. Tricuspid annular displacement predicts survival in pulmonary hypertension. *Am J Respir Crit Care Med* 2006;**174**:1034–1041.
4. Haddad F, Doyle R, Murphy DJ, Hunt SA. Right ventricular function in cardiovascular disease, part II: pathophysiology, clinical importance, and management of right ventricular failure. *Circulation* 2008;**117**:1717–1731.
5. Meyer P, Filippatos GS, Ahmed MI, Iskandrian AE, Bittner V, Perry GJ, White M, Aban IB, Mujib M, Dell'Italia LJ, Ahmed A. Effects of right ventricular ejection fraction on outcomes in chronic systolic heart failure. *Circulation* 2010;**121**:252–258.
6. de Groote P, Millaire A, Foucher-Hossein C, Nugue O, Marchandise X, Ducloux G, Lablanche J-M. Right ventricular ejection fraction is an independent predictor of survival in patients with moderate heart failure. *J Am Coll Cardiol* 1998;**32**:948–954.
7. Mertens LL, Friedberg MK. Imaging the right ventricle—current state of the art. *Nat Rev Cardiol* 2010;**7**:551–563.
8. Haddad F, Hunt SA, Rosenthal DN, Murphy DJ. Right ventricular function in cardiovascular disease, part I: anatomy, physiology, aging, and functional assessment of the right ventricle. *Circulation* 2008;**117**:1436–1448.
9. Foale R, Nihoyannopoulos P, McKenna W, Kleinebenne A, Nadazdin A, Rowland E, Smith G. Echocardiographic measurement of the normal adult right ventricle. *Br Heart J* 1986;**56**:33–44.
10. Sheehan FH, Ge S, Vick GW 3rd, Urnes K, Kerwin WS, Bolson EL, Chung T, Kovalchin JP, Sahn DJ, Jerosch-Herold M, Stolpen AH. Three-dimensional shape analysis of right ventricular remodeling in repaired tetralogy of Fallot. *Am J Cardiol* 2008;**101**:107–113.
11. Anderson RH, Ho SY. Sequential segmental analysis: description and characterization for the millenium. *Cardiol Young* 1997;**7**:98–116.
12. Sengupta PP, Korinek J, Belohlavek M, Narula J, Vannan MA, Jahangir A, Khandheria BK. Left ventricular structure and function: basic science for cardiac imaging. *J Am Coll Cardiol* 2006;**48**:1988–2001.
13. Sengupta PP, Krishnamoorthy VK, Korinek J, Narula J, Vannan MA, Lester SJ, Tajik JA, Seward JB, Khandheria BK, Belohlavek M. Left ventricular form and function revisited: applied translational science to cardiovascular ultrasound imaging. *J Am Soc Echocardiogr* 2007;**20**:539–551.
14. Haber I, Metaxas DN, Geva T, Axel L. Three-dimensional systolic kinematics of the right ventricle. *Am J Physiol Heart Circ Physiol* 2005;**289**:H1826–H1833.
15. Sanchez-Quintana D, Anderson RH, Ho SY. Ventricular myoarchitecture in tetralogy of Fallot. *Heart* 1996;**76**:280–286.
16. Pettersen E, Helle-Valle T, Edvardsen T, Lindberg H, Smith HJ, Smevik B, Smiseth OA, Andersen K. Contraction pattern of the systemic right ventricle shift from longitudinal to circumferential shortening and absent global ventricular torsion. *J Am Coll Cardiol* 2007;**49**:2450–2456.
17. Bishop A, White P, Oldershaw P, Chaturvedi R, Brookes C, Redington A. Clinical application of the conductance catheter technique in the adult human right ventricle. *Int J Cardiol* 1997;**58**:211–221.
18. Redington AN, Rigby ML, Shinebourne EA, Oldershaw PJ. Changes in the pressure-volume relation of the right ventricle when its loading conditions are modified. *Br Heart J* 1990;**63**:45–49.
19. Sheehan F, Redington A. The right ventricle: anatomy, physiology and clinical imaging. *Heart* 2008;**94**:1510–1515.
20. Bogaard HJ, Abe K, Vonk Noordegraaf A, Voelkel NF. The right ventricle under pressure: cellular and molecular mechanisms of right-heart failure in pulmonary hypertension. *Chest* 2009;**135**:794–804.
21. Kaufman BD, Desai M, Reddy S, Osorio JC, Chen JM, Mosca RS, Ferrante AW, Mital S. Genomic profiling of left and right ventricular hypertrophy in congenital heart disease. *J Card Fail* 2008;**14**:760–767.
22. Mital S. Right ventricle in congenital heart disease: is it just a 'weaker' left ventricle? *Arch Mal Coeur Vaiss* 2006;**99**:1244–1251.
23. Rochais F, Mesbah K, Kelly RG. Signaling pathways controlling second heart field development. *Circ Res* 2009;**104**:933–942.
24. Zaffran S, Kelly RG, Meilhac SM, Buckingham ME, Brown NA. Right ventricular myocardium derives from the anterior heart field. *Circ Res* 2004;**95**:261–268.
25. Puwanant S, Park M, Popovic ZB, Tang WH, Farha S, George D, Sharp J, Puntawangkoon J, Loyd JE, Erzurum SC, Thomas JD. Ventricular geometry, strain, and rotational mechanics in pulmonary hypertension. *Circulation* 2010;**121**:259–266.
26. Raymond RJ, Hinderliter AL, Willis PW, Ralph D, Caldwell EJ, Williams W, Ettinger NA, Hill NS, Summer WR, de Boisblanc B, Schwartz T, Koch G, Clayton LM, Jobsis MM, Crow JW, Long W. Echocardiographic predictors of adverse outcomes in primary pulmonary hypertension. *J Am Coll Cardiol* 2002;**39**:1214–1219.
27. Stojnic BB, Brecker SJ, Xiao HB, Helmy SM, Mbaissouroum M, Gibson DG. Left ventricular filling characteristics in pulmonary hypertension: a new mode of ventricular interaction. *Br Heart J* 1992;**68**:16–20.
28. Walker RE, Moran AM, Gauvreau K, Colan SD. Evidence of adverse ventricular interdependence in patients with atrial septal defects. *Am J Cardiol* 2004;**93**:1374–1377, A6.
29. Rudski LG, Lai WW, Afilalo J, Hua L, Handschumacher MD, Chandrasekaran K, Solomon SD, Louie EK, Schiller NB. Guidelines for the echocardiographic assessment of the right heart in adults: a report from the American Society of Echocardiography endorsed by the European Association of Echocardiography, a registered branch of the European Society of Cardiology, and the Canadian Society of Echocardiography. *J Am Soc Echocardiogr* 2010;**23**:685–713; quiz 786–788.
30. Lopez L, Colan SD, Frommelt PC, Ensing GJ, Kendall K, Younoszai AK, Lai WW, Geva T. Recommendations for quantification methods during the performance of a pediatric echocardiogram: a report from the Pediatric Measurements Writing Group of the American Society of Echocardiography Pediatric and Congenital Heart Disease Council. *J Am Soc Echocardiogr* 2010;**23**:465–495; quiz 576–577.
31. Lai WW, Gauvreau K, Rivera ES, Saleeb S, Powell AJ, Geva T. Accuracy of guideline recommendations for two-dimensional quantification of the right ventricle by echocardiography. *Int J Cardiovasc Imaging* 2008;**24**:691–698.
32. Helbing WA, Bosch HG, Maliepaard C, Rebergen SA, van der Geest RJ, Hansen B, Ottenkamp J, Reiber JH, de Roos A. Comparison of echocardiographic methods with magnetic resonance imaging for assessment of right ventricular function in children. *Am J Cardiol* 1995;**76**:589–594.
33. Shimada YJ, Shiota M, Siegel RJ, Shiota T. Accuracy of right ventricular volumes and function determined by three-dimensional echocardiography in comparison with magnetic resonance imaging: a meta-analysis study. *J Am Soc Echocardiogr* 2010;**23**:943–953.
34. Grewal J, Majdalany D, Syed I, Pellikka P, Warnes CA. Three-dimensional echocardiographic assessment of right ventricular volume and function in adult patients with congenital heart disease: comparison with magnetic resonance imaging. *J Am Soc Echocardiogr* 2010;**23**:127–133.
35. Niemann PS, Pinho L, Balbach T, Galuschky C, Blankenhagen M, Silberbach M, Broberg C, Jerosch-Herold M, Sahn DJ. Anatomically oriented right ventricular volume measurements with dynamic three-dimensional echocardiography validated by 3-Tesla magnetic resonance imaging. *J Am Coll Cardiol* 2007;**50**:1668–1676.

36. van der Zwaan HB, Geleijnse ML, Soliman OI, McGhie JS, Wiegers-Groeneweg EJ, Helbing WA, Roos-Hesselink JW, Meijboom FJ. Test-retest variability of volumetric right ventricular measurements using real-time three-dimensional echocardiography. *J Am Soc Echocardiogr* 2011;**24**:671–679.

37. van der Zwaan HB, Helbing WA, Boersma E, Geleijnse ML, McGhie JS, Soliman OI, Roos-Hesselink JW, Meijboom FJ. Usefulness of real-time three-dimensional echocardiography to identify right ventricular dysfunction in patients with congenital heart disease. *Am J Cardiol* 2010;**106**:843–850.

38. van der Zwaan HB, Helbing WA, McGhie JS, Geleijnse ML, Luijnenburg SE, Roos-Hesselink JW, Meijboom FJ. Clinical value of real-time three-dimensional echocardiography for right ventricular quantification in congenital heart disease: validation with cardiac magnetic resonance imaging. *J Am Soc Echocardiogr* 2010;**23**:134–140.

39. Khoo NS, Young A, Occleshaw C, Cowan B, Zeng IS, Gentles TL. Assessments of right ventricular volume and function using three-dimensional echocardiography in older children and adults with congenital heart disease: comparison with cardiac magnetic resonance imaging. *J Am Soc Chocardiogr* 2009;**22**:1279–1288.

40. Takahashi K, Inage A, Rebeyka IM, Ross DB, Thompson RB, Mackie AS, Smallhorn JF. Real-time 3-dimensional echocardiography provides new insight into mechanisms of tricuspid valve regurgitation in patients with hypoplastic left heart syndrome. *Circulation* 2009;**120**:1091–1098.

41. Nii M, Guerra V, Roman KS, Macgowan CK, Smallhorn JF. Three-dimensional tricuspid annular function provides insight into the mechanisms of tricuspid valve regurgitation in classic hypoplastic left heart syndrome. *J Am Soc Echocardiogr* 2006;**19**:391–402.

42. Nii M, Roman KS, Macgowan CK, Smallhorn JF. Insight into normal mitral and tricuspid annular dynamics in pediatrics: a real-time three-dimensional echocardiographic study. *J Am Soc Echocardiogr* 2005;**18**:805–814.

43. Anavekar NS, Gerson D, Skali H, Kwong RY, Yucel EK, Solomon SD. Two-dimensional assessment of right ventricular function: an echocardiographic-MRI correlative study. *Echocardiography* 2007;**24**:452–456.

44. Tei C, Nishimura RA, Seward JB, Tajik AJ. Noninvasive Doppler-derived myocardial performance index: correlation with simultaneous measurements of cardiac catheterization measurements. *J Am Soc Echocardiogr* 1997;**10**:169–178.

45. Cheung MM, Smallhorn JF, Redington AN, Vogel M. The effects of changes in loading conditions and modulation of inotropic state on the myocardial performance index: comparison with conductance catheter measurements. *Eur Heart J* 2004;**25**:2238–2242.

46. Dragulescu A, Mertens LL. Developments in echocardiographic techniques for the evaluation of ventricular function in children. *Arch Cardiovasc Dis* 2010;**103**:603–614.

47. Dambrauskaite V, Delcroix M, Claus P, Herbots L, D'Hooge J, Bijnens B, Rademakers F, Sutherland GR. Regional right ventricular dysfunction in chronic pulmonary hypertension. *J Am Soc Echocardiogr* 2007;**20**:1172–1180.

48. Giusca S, Dambrauskaite V, Scheurwegs C, D'Hooge J, Claus P, Herbots L, Magro M, Rademakers F, Meyns B, Delcroix M, Voigt JU. Deformation imaging describes right ventricular function better than longitudinal displacement of the tricuspid ring. *Heart* 2010;**96**:281–288.

49. Bos JM, Hagler DJ, Silvilairat S, Cabalka A, O'Leary P, Daniels O, Miller FA, Abraham TP. Right ventricular function in asymptomatic individuals with a systemic right ventricle. *J Am Soc Echocardiogr* 2006;**19**:1033–1037.

50. Eyskens B, Weidemann F, Kowalski M, Bogaert J, Dymarkowski S, Bijnens B, Gewillig M, Sutherland G, Mertens L. Regional right and left ventricular function after the Senning operation: an ultrasonic study of strain rate and strain. *Cardiol Young* 2004;**14**:255–264.

51. Eyskens B, Brown SC, Claus P, Dymarkowski S, Gewillig M, Bogaert J, Mertens L. The influence of pulmonary regurgitation on regional right ventricular function in children after surgical repair of tetralogy of Fallot. *Eur J Echocardiogr* 2010;**11**:341–345.

52. Weidemann F, Eyskens B, Mertens L, Dommke C, Kowalski M, Simmons L, Claus P, Bijnens B, Gewillig M, Hatle L, Sutherland GR. Quantification of regional right and left ventricular function by ultrasonic strain rate and strain indexes after surgical repair of tetralogy of Fallot. *Am J Cardiol* 2002;**90**:133–138.

53. Koopman LP, Slorach C, Hui W, Manlhiot C, McCrindle BW, Friedberg MK, Jaeggi ET, Mertens L. Comparison between different speckle tracking and color tissue Doppler techniques to measure global and regional myocardial deformation in children. *J Am Soc Echocardiogr* 2010;**23**:919–928.

54. Greil GF, Boettger T, Germann S, Klumpp B, Baltes C, Kozerke S, Bialkowski A, Urschitz MS, Miller S, Wolf I, Meinzer H-P, Sieverding L. Quantitative assessment of ventricular function using three-dimensional SSFP magnetic resonance angiography. *J Magn Reson Imaging* 2007;**26**:288–295.

55. Valsangiacomo Büchel ER, DiBernardo S, Bauersfeld U, Berger F. Contrast-enhanced magnetic resonance angiography of the great arteries in patients with congenital heart disease: an accurate tool for planning catheter-guided interventions. *Int J Cardiovasc Imaging* 2005;**21**:313–322.

56. Beroukhim RS, Prakash A, Valsangiacomo Buechel ER, Cava JR, Dorfman AL, Festa P, Hlavacek AM, Johnson TR, Keller MS, Krishnamurthy R, Misra N, Moniotte S, Parks WJ, Powell AJ, Soriano BD, Srichai MB, Yoo S-J, Zhou J, Geva T. Characterization of cardiac tumors in children by cardiovascular magnetic resonance imaging: a multicenter experience. *J Am Coll Cardiol* 2011;**58**:1044–1054.

57. Marcus FI, McKenna WJ, Sherrill D, Basso C, Bauce B, Bluemke DA, Calkins H, Corrado D, Cox MGPJ, Daubert JP, Fontaine G, Gear K, Hauer R, Nava A, Picard MH, Protonotarios N, Saffitz JE, Sanborn DMY, Steinberg JS, Tandri H, Thiene G, Towbin JA, Tsatsopoulou A, Wichter T, Zareba W. Diagnosis of arrhythmogenic right ventricular cardiomyopathy/dysplasia. *Eur Heart J* 2010;**31**:806–814.

58. Mahrholdt H, Wagner A, Judd RM, Sechtem U, Kim RJ. Delayed enhancement cardiovascular magnetic resonance assessment of non-ischaemic cardiomyopathies. *Eur Heart J* 2005;**26**:1461–1474.

59. Masci PG, Francone M, Desmet W, Ganame J, Todiere G, Donato R, Siciliano V, Carbone I, Mangia M, Strata E, Catalano C, Lombardi M, Agati L, Janssens S, Bogaert J. Right ventricular ischemic injury in patients with acute ST-segment elevation myocardial infarction/clinical perspective. *Circulation* 2010;**122**:1405–1412.

60. Babu-Narayan SV, Goktekin O, Moon JC, Broberg CS, Pantely GA, Pennell DJ, Gatzoulis MA, Kilner PJ. Late gadolinium enhancement cardiovascular magnetic resonance of the systemic right ventricle in adults with previous atrial redirection surgery for transposition of the great arteries. *Circulation* 2005;**111**:2091–2098.

61. Babu-Narayan SV, Kilner PJ, Li W, Moon JC, Goktekin O, Davlouros PA, Khan M, Ho SY, Pennell DJ, Gatzoulis MA. Ventricular fibrosis suggested by cardiovascular magnetic resonance in adults with repaired tetralogy of Fallot and its relationship to adverse markers of clinical outcome. *Circulation* 2006;**113**:405–413.

62. Miller S, Simonetti O, Carr J, Kramer U, Finn J. MR Imaging of the heart with cine true fast imaging with steady-state precession: influence of spatial and temporal resolutions on left ventricular functional parameters. *Radiology* 2002;**223**:263–269.

63. Maceira A, Prasad S, Khan M, Pennell D. Reference right ventricular systolic and diastolic function normalized to age, gender and body surface area from steady-state free precession cardiovascular magnetic resonance. *Eur Heart J* 2006;**27**:2879–2888.

64. Buechel E, Kaiser T, Jackson C, Schmitz A, Kellenberger C. Normal right- and left ventricular volumes and myocardial mass in children measured by steady state free precession cardiovascular magnetic resonance. *J Cardiovasc Magn Reson* 2009;**11**:19.

65. Sarikouch S, Peters B, Gutberlet M, Leismann B, Kelter-Kloepping A, Koerperich H, Kuehne T, Beerbaum P. Sex-specific pediatric percentiles for ventricular size and mass as reference values for cardiac MRI/clinical perspective. *Circulation* 2010;**3**:65–76.

66. Buechel ERV, Dave HH, Kellenberger CJ, Dodge-Khatami A, Pretre R, Berger F, Bauersfeld U. Remodelling of the right ventricle after early pulmonary valve replacement in children with repaired tetralogy of Fallot: assessment by cardiovascular magnetic resonance. *Eur Heart J* 2005;**26**:2721–2727.

67. Grothues F, Moon J, Bellenger N, Smith G, Klein H, Pennell D. Interstudy reproducibility of right ventricular volumes, function, and mass with cardiovascular magnetic resonance. *Am Heart J* 2004;**147**:218–223.

68. Fratz S, Schuhbaeck A, Buchner C, Busch R, Meierhofer C, Martinoff S, Hess J, Stern H. Comparison of accuracy of axial slices versus short-axis slices for measuring ventricular volumes by cardiac magnetic resonance in patients with corrected tetralogy of Fallot. *Am J Cardiol* 2009;**103**:1764–1769.

69. Robbers-Visser DL, Luijnenburg SE, van den Berg J, Moelker A, Helbing WA. Stress imaging in congenital cardiac disease. *Cardiol Young* 2009;**19**:552–562.

70. Greil GF, Beerbaum P, Razavi R, Miller O. Imaging the right ventricle. *Heart* 2008;**94**:803–808.

71. Youssef A, Ibrahim E-S, Korosoglou G, Abraham MR, Weiss R, Osman N. Strain-encoding cardiovascular magnetic resonance for assessment of right-ventricular regional function. *J Cardiovasc Magn Reson* 2008;**10**:33.

72. Menteer JWP, Fogel MA. Quantifying regional right ventricular function in tetralogy of Fallot. *J Cardiovasc Magn Reson* 2005;**7**:753–761.

73. Wald RM, Redington AN, Pereira A, Provost YL, Paul NS, Oechslin EN, Silversides CK. Refining the assessment of pulmonary regurgitation in adults after tetralogy of Fallot repair: should we be measuring regurgitant fraction or regurgitant volume? *Eur Heart J* 2009;**30**:356–361.

74. Roman KS, Kellenberger CJ, Farooq S, MacGowan CK, Gilday DL, Yoo S-J. Comparative imaging of differential pulmonary blood flow in patients with congenital heart disease: magnetic resonance imaging versus lung perfusion scintigraphy. *Pediatr Radiol* 2005;**35**:295–301.

75. Beerbaum P, Körperich H, Barth P, Esdorn H, Gieseke J, Meyer H. Noninvasive quantification of left-to-right shunt in pediatric patients: phase-contrast cine magnetic resonance imaging compared with invasive oximetry. *Circulation* 2001;**103**:2476–2482.

76. Dupont MIVM, Drägean CA, Coche EE. Right ventricle function assessment by MDCT. *AJR* 2011;**196**:77–86.

77. Ghaye B, Ghuysen A, Bruyere P-J, D' Orio V, Dondelinger RF. Can CT pulmonary angiography allow assessment of severity and prognosis in patients presenting with pulmonary embolism? What the radiologist needs to know. *RadioGraphics* 2006;**26**:23–39.

78. Andreini D, Pontone G, Bartorelli AL, Agostoni P, Mushtaq S, Bertella E, Trabattoni D, Cattadori G, Cortinovis S, Annoni A, Castelli A, Ballerini G, Pepi M. Sixty-four-slice multidetector computed tomography/CLINICAL PERSPECTIVE. *Circ Cardiovasc Imaging* 2009;**2**:199–205.

79. Andreini D, Pontone G, Pepi M, Ballerini G, Bartorelli AL, Magini A, Quaglia C, Nobili E, Agostoni P. Diagnostic accuracy of multidetector computed tomography coronary angiography in patients with dilated cardiomyopathy. *J Am Coll Cardiol* 2007;**49**:2044–2050.

80. Herzog BA, Wyss CA, Husmann L, Gaemperli O, Valenta I, Treyer V, Landmesser U, Kaufmann PA. First head-to-head comparison of effective radiation dose from low-dose 64-slice CT with prospective ECG-triggering versus invasive coronary angiography. *Heart* 2009;**95**:1656–1661.

81. Revel M-P, Faivre J-B, Remy-Jardin M, Delannoy-Deken Vr, Duhamel A, Remy J. Pulmonary hypertension: ECG-gated 64-section CT angiographic evaluation of new functional parameters as diagnostic criteria. *Radiology* 2009;**250**:558–566.

82. Lin FY, Devereux RB, Roman MJ, Meng J, Jow VM, Jacobs A, Weinsaft JW, Shaw LJ, Berman DS, Callister TQ, Min JK. Cardiac chamber volumes, function, and mass as determined by 64-multidetector row computed tomography: mean values among healthy adults free of hypertension and obesity. *JACC Cardiovasc Imaging* 2008;**1**:782–786.

83. Plumhans Cd, Muehlenbruch G, Rapaee A, Sim K-H, Seyfarth T, Gaenther RW, Mahnken AH. Assessment of global right ventricular function on 64-MDCT compared with MRI. *AJR* 2008;**190**:1358–1361.

84. Rich JD, Ward RP. Right-ventricular function by nuclear cardiology. *Curr Opin Cardiol* 2010;**25**:445–450. doi:10.1097/HCO.0b013e32833cb252.

85. Ramani G, Gurm G, Dilsizian V, Park M. Noninvasive assessment of right ventricular function: will there be resurgence in radionuclide imaging techniques. *Curr Cardiol Rep* 2010;**12**:162–169.

86. Daou DVKS, Coaquila C, Lebtahi R, Fourme T, Sitbon O, Parent F, Slama M, Le Guludec D, Simonneau G. Automatic quantification of right ventricular function with gated blood pool SPECT. *J Nucl Cardiol* 2004;**11**:293–304.

87. Nichols KSR, Ababneh AA, Barst RJ, Rosenbaum MS, Groch MW, Shoyeb AH, Bergmann SR. Validation of SPECT equilibrium radionuclide angiographic right ventricular parameters by cardiac magnetic resonance imaging. *J Nucl Cardiol* 2002;**9**:153–160.

88. Nagaya N, Goto Y, Satoh T, Uematsu S, Hamada S, Kuribayashi S, Okano Y, Kyotani S, Shimotsu Y, Fukuchi K, Nakanishi N, Takamiya M, Ishida Y. Impaired regional fatty acid uptake and systolic dysfunction in hypertrophied right ventricle. *J Nucl Med* 1998;**39**:1676–1680.

89. Oikawa M, Kagaya Y, Otani H, Sakuma M, Demachi J, Suzuki J, Takahashi T, Nawata J, Ido T, Watanabe J, Shirato K. Increased [18F]fluorodeoxyglucose accumulation in right ventricular free wall in patients with pulmonary hypertension and the effect of epoprostenol. *J Am Coll Cardiol* 2005;**45**:1849–1855.

90. Gaemperli O, Bengel FM, Kaufmann PA. Cardiac hybrid imaging. *Eur Heart J* 2011;**32**:2100–2108.

91. Torbicki A, Perrier A, Konstantinides S, Agnelli G, Galie N, Pruszczyk P, Bengel F, Brady AJ, Ferreira D, Janssens U, Klepetko W, Mayer E, Remy-Jardin M, Bassand JP. Guidelines on the diagnosis and management of acute pulmonary embolism: the Task Force for the Diagnosis and Management of Acute Pulmonary Embolism of the European Society of Cardiology (ESC). *Eur Heart J* 2008;**29**:2276–2315.

92. Badesch DB, Champion HC, Sanchez MA, Hoeper MM, Loyd JE, Manes A, McGoon M, Naeije R, Olschewski H, Oudiz RJ, Torbicki A. Diagnosis and assessment of pulmonary arterial hypertension. *J Am Coll Cardiol* 2009;**54**(1 Suppl):S55–S66.

93. Thenappan T, Shah SJ, Rich S, Tian L, Archer SL, Gomberg-Maitland M. Survival in pulmonary arterial hypertension: a reappraisal of the NIH risk stratification equation. *Eur Respir J* 2010;**35**:1079–1087.

94. Ghio S, Klersy C, Magrini G, D'Armini AM, Scelsi L, Raineri C, Pasotti M, Serio A, Campana C, Vigano M. Prognostic relevance of the echocardiographic assessment of right ventricular function in patients with idiopathic pulmonary arterial hypertension. *Int J Cardiol* 2010;**140**:272–278.

95. Grapsa J, O'Regan DP, Pavlopoulos H, Durighel G, Dawson D, Nihoyannopoulos P. Right ventricular remodelling in pulmonary arterial hypertension with three-dimensional echocardiography: comparison with cardiac magnetic resonance imaging. *Eur J Echocardiogr* 2010;**11**:64–73.

96. Benza R, Biederman R, Murali S, Gupta H. Role of cardiac magnetic resonance imaging in the management of patients with pulmonary arterial hypertension. *J Am Coll Cardiol* 2008;**52**:1683–1692.

97. Shehata ML, Lossnitzer D, Skrok J, Boyce D, Lechtzin N, Mathai SC, Girgis RE, Osman N, Lima JA, Bluemke DA, Hassoun PM, Vogel-Claussen J. Myocardial delayed enhancement in pulmonary hypertension: pulmonary hemodynamics, right ventricular function, and remodeling. *AJR* 2011;**196**:87–94.

98. Fernandez-Friera L, Garcia-Alvarez A, Guzman G, Bagheriannejad-Esfahani F, Malick W, Nair A, Fuster V, Garcia MJ, Sanz J. Apical right ventricular dysfunction in patients with pulmonary hypertension demonstrated with magnetic resonance. *Heart* 2011;**97**:1250–1256.

99. Douma RA, Kamphuisen PW, Buller HR. Acute pulmonary embolism. Part 1: epidemiology and diagnosis. *Nat Rev Cardiol* 2010;**7**:585–596.

100. Value of the ventilation/perfusion scan in acute pulmonary embolism. Results of the prospective investigation of pulmonary embolism diagnosis (PIOPED). The PIOPED Investigators. *JAMA* 1990;**263**:2753–2759.

101. Roy PM, Colombet I, Durieux P, Chatellier G, Sors H, Meyer G. Systematic review and meta-analysis of strategies for the diagnosis of suspected pulmonary embolism. *BMJ* 2005;**331**:259.

102. ten Wolde M, Sohne M, Quak E, Mac Gillavry MR, Buller HR. Prognostic value of echocardiographically assessed right ventricular dysfunction in patients with pulmonary embolism. *Arch Intern Med* 2004;**164**:1685–1689.

103. Andersen HR, Falk E, Nielsen D. Right ventricular infarction: frequency, size and topography in coronary heart disease: a prospective study comprising 107 consecutive autopsies from a coronary care unit. *J Am Coll Cardiol* 1987;**10**:1223–1232.

104. Dell'Italia LJ, Starling MR, Crawford MH, Boros BL, Chaudhuri TK, O'Rourke RA. Right ventricular infarction: identification by hemodynamic measurements before and after volume loading and correlation with noninvasive techniques. *J Am Coll Cardiol* 1984;**4**:931–939.

105. Lopez-Sendon J, Garcia-Fernandez MA, Coma-Canella I, Yangüela MM, Bañuelos F. Segmental right ventricular function after acute myocardial infarction: two-dimensional echocardiographic study in 63 patients. *Am J Cardiol* 1983;**51**:390–396.

106. Alam M, Wardell J, Andersson E, Samad BA, Nordlander R. Right ventricular function in patients with first inferior myocardial infarction: assessment by tricuspid annular motion and tricuspid annular velocity. *Am Heart J* 2000;**139**:710–715.

107. Kakouros N, Cokkinos DV. Right ventricular myocardial infarction: pathophysiology, diagnosis, and management. *Postgrad Med J* 2010;**86**:719–728.

108. Kim HW, Farzaneh-Far A, Kim RJ. Cardiovascular magnetic resonance in patients with myocardial infarction: current and emerging applications. *J Am Coll Cardiol* 2009;**55**:1–16.

109. Manka R, Fleck E, Paetsch I. Silent inferior myocardial infarction with extensive right ventricular scarring. *Int J Cardiol* 2008;**127**:e186–e187.

110. Kumar A, Abdel-Aty H, Kriedemann I, Schulz-Menger J, Gross CM, Dietz R, Friedrich MG. Contrast-enhanced cardiovascular magnetic resonance imaging of right ventricular infarction. *J Am Coll Cardiol* 2006;**48**:1969–1976.

111. Larose E, Ganz P, Reynolds HG, Dorbala S, Di Carli MF, Brown KA, Kwong RY. Right ventricular dysfunction assessed by cardiovascular magnetic resonance imaging predicts poor prognosis late after myocardial infarction. *J Am Coll Cardiol* 2007;**49**:855–862.

112. Juillière Y, Barbier G, Feldmann L, Grentzinger A, Danchin N, Cherrier F. Additional predictive value of both left and right ventricular ejection fractions on long-term survival in idiopathic dilated cardiomyopathy. *Eur Heart J* 1997;**18**:276–280.

113. Carbone I, Francone M, Chimenti C, Galea N, Russo M, Frustaci A. Right ventricular late enhancement as a magnetic resonance marker of glycogen storage disease. *Circulation* 2010;**122**:189–190.

114. Mahrholdt H, Wagner A, Deluigi CC, Kispert E, Hager S, Meinhardt G, Vogelsberg H, Fritz P, Dippon J, Bock C-T, Klingel K, Kandolf R, Sechtem U. Presentation, patterns of myocardial damage, and clinical course of viral myocarditis. *Circulation* 2006;**114**:1581–1590.

115. Basso C, Corrado D, Marcus Fl, Nava A, Thiene G. Arrhythmogenic right ventricular cardiomyopathy. *Lancet* 2009;**373**:1289–1300.

116. Yoerger DM, Marcus F, Sherrill D, Calkins H, Towbin JA, Zareba W, Picard MH. Echocardiographic findings in patients meeting task force criteria for arrhythmogenic right ventricular dysplasia: new insights from the multidisciplinary study of right ventricular dysplasia. *J Am Coll Cardiol* 2005;**45**:860–865.

117. Prakasa KR, Dalal D, Wang J, Bomma C, Tandri H, Dong J, James C, Tichnell C, Russell SD, Spevak P, Corretti M, Bluemke DA, Calkins H, Abraham TP. Feasibility and variability of three dimensional echocardiography in arrhythmogenic right ventricular dysplasia/cardiomyopathy. *Am J Cardiol* 2006;**97**:703–709.

118. Prakasa KR, Wang J, Tandri H, Dalal D, Bomma C, Chojnowski R, James C, Tichnell C, Russell S, Judge D, Corretti M, Bluemke D, Calkins H, Abraham TP. Utility of tissue Doppler and strain echocardiography in arrhythmogenic right ventricular dysplasia/cardiomyopathy. *Am J Cardiol* 2007;**100**: 507–512.

119. Tandri H, Castillo E, Ferrari VA, Nasir K, Dalal D, Bomma C, Calkins H, Bluemke DA. Magnetic resonance imaging of arrhythmogenic right ventricular dysplasia: sensitivity, specificity, and observer variability of fat detection versus functional analysis of the right ventricle. *J Am Coll Cardiol* 2006;**48**:2277–2284.

120. Tandri H, Macedo R, Calkins H, Marcus F, Cannom D, Scheinman M, Daubert J, Estes Iii M, Wilber D, Talajic M, Duff H, Krahn A, Sweeney M, Garan H, Bluemke DA. Role of magnetic resonance imaging in arrhythmogenic right ventricular dysplasia: insights from the North American arrhythmogenic right ventricular dysplasia (ARVD/C) study. *Am Heart J* 2008;**155**:147–153.

121. Oechslin EN, Harrison DA, Harris L, Downar E, Webb GD, Siu SS, Williams WG. Reoperation in adults with repair of tetralogy of Fallot: indications and outcomes. *J Thorac Cardiovasc Surg* 1999;**118**:245–251.

122. Greutmann M, Tobler D, Biaggi P, Mah ML, Crean A, Oechslin EN, Silversides CK. Echocardiography for assessment of right ventricular volumes revisited: a cardiac magnetic resonance comparison study in adults with repaired tetralogy of Fallot. *J Am Soc Echocardiogr* 2010;**23**:905–911.

123. Gatzoulis MA, Clark AL, Cullen S, Newman CG, Redington AN. Right ventricular diastolic function 15 to 35 years after repair of tetralogy of Fallot. Restrictive physiology predicts superior exercise performance. *Circulation* 1995;**91**: 1775–1781.

124. Geva T. Indications and timing of pulmonary valve replacement after tetralogy of Fallot repair. *Semin Thorac Cardiovasc Surg* 2006;**9**:11–22.

125. Therrien J, Provost Y, Merchant N, Williams W, Colman J, Webb G. Optimal timing for pulmonary valve replacement in adults after tetralogy of Fallot repair. *Am J Cardiol* 2005;**95**:779–782.

126. Oosterhof T, van Straten A, Vliegen HW, Meijboom FJ, van Dijk APJ, Spijkerboer AM, Bouma BJ, Zwinderman AH, Hazekamp MG, de Roos A, Mulder BJM. Preoperative thresholds for pulmonary valve replacement in patients with corrected tetralogy of Fallot using cardiovascular magnetic resonance. *Circulation* 2007;**116**:545–551.

127. Knirsch W, Dodge-Khatami A, Kadner A, Kretschmar O, Steiner J, Böttler P, Kececioglu D, Harpes P, Valsangiacomo Buechel E. Assessment of myocardial function in pediatric patients with operated tetralogy of Fallot: preliminary results with 2D strain echocardiography. *Pediatr Cardiol* 2008;**29**:718–725.

128. Kempny A, Diller G-P, Orwat S, Kaleschke G, Kerckhoff G, Bunck AC, Maintz D, Baumgartner H. Right ventricular-left ventricular interaction in adults with Tetralogy of Fallot: a combined cardiac magnetic resonance and echocardiographic speckle tracking study. *Int J Cardiol* 2010; in press.

129. Moiduddin N, Asoh K, Slorach C, Benson LN, Friedberg MK. Effect of transcatheter pulmonary valve implantation on short-term right ventricular function as determined by two-dimensional speckle tracking strain and strain rate imaging. *Am J Cardiol* 2009;**104**:862–867.

130. van der Hulst AE, Roest AAW, Delgado V, Kroft LJM, Holman ER, Blom NA, Bax JJ, de Roos A, Westenberg JJM. Corrected tetralogy of Fallot: comparison of tissue doppler imaging and velocity-encoded MR for assessment of performance and temporal activation of right ventricle. *Radiology* 2011;**260**:88–97.

131. Bodhey NK, Beerbaum P, Sarikouch S, Kropf S, Lange P, Berger F, Anderson RH, Kuehne T. Functional analysis of the components of the right ventricle in the setting of tetralogy of Fallot/CLINICAL PERSPECTIVE. *Circ Cardiovasc Imaging* 2008;**1**:141–147.

132. Wald RM, Haber I, Wald R, Valente AM, Powell AJ, Geva T. Effects of regional dysfunction and late gadolinium enhancement on global right ventricular function and exercise capacity in patients with repaired tetralogy of Fallot. *Circulation* 2009;**119**:1370–1377.

133. Caputo GR, Kondo C, Masui T, Geraci SJ, Foster E, O'Sullivan MM, Higgins CB. Right and left lung perfusion: in vitro and in vivo validation with oblique-angle, velocity-encoded cine MR imaging. *Radiology* 1991;**180**:693–698.

134. Oosterhof T, Mulder BJM, Vliegen HW, de Roos A. Corrected tetralogy of Fallot: delayed enhancement in right ventricular outflow tract. *Radiology* 2005; **237**:868–871.

135. Schievano SCL, Migliavacca F, Norman W, Frigiola A, Deanfield J, Bonhoeffer P, Taylor AM. Variations in right ventricular outflow tract morphology following repair of congenital heart disease: implications for percutaneous pulmonary valve implantation. *J Cardiovasc Magn Reson* 2007;**9**:687–695.

136. Raymond RJ, Hinderliter AL, Willis PW, Ralph D, Caldwell EJ, Williams W, Ettinger NA, Hill NS, Summer WR, de Boisblanc B, Schwartz T, Koch G, Clayton LM, Jöbsis MM, Crow JW, Long W. Echocardiographic predictors of adverse outcomes in primary pulmonary hypertension. *J Am Coll Cardiol* 2002; **39**:1214–1219.

137. Ghio S, Pazzano AS, Klersy C, Scelsi L, Raineri C, Camporotondo R, D'Armini A, Visconti LO. Clinical and prognostic relevance of echocardiographic evaluation of right ventricular geometry in patients with idiopathic pulmonary arterial hypertension. *Am J Cardiol* 2011;**107**:628–632.

138. Yeo TC, Dujardin KS, Tei C, Mahoney DW, McGoon MD, Seward JB. Value of a Doppler-derived index combining systolic and diastolic time intervals in predicting outcome in primary pulmonary hypertension. *Am J Cardiol* 1998;**81**:1157–1161.

139. Mahapatra S, Nishimura RA, Sorajja P, Cha S, McGoon MD. Relationship of pulmonary arterial capacitance and mortality in idiopathic pulmonary arterial hypertension. *J Am Coll Cardiol* 2006;**47**:799–803.

140. Mahapatra S, Nishimura RA, Oh JK, McGoon MD. The prognostic value of pulmonary vascular capacitance determined by Doppler echocardiography in patients with pulmonary arterial hypertension. *J Am Soc Echocardiogr* 2006;**19**: 1045–1050.

141. Sachdev A, Villarraga HR, Frantz RP, McGoon MD, Hsiao JF, Maalouf JF, Ammash NM, McCully RB, Miller FA, Pellikka PA, Oh JK, Kane GC. Right ventricular strain for prediction of survival in patients with pulmonary arterial hypertension. *Chest* 2011;**139**:1299–1309.